Article ID:1004-4213(2010)02-0233-5

Modeling of the Radiation Impedance Characteristics for Photoconductive Antenna*

XU Ying[1], CHEN Hai-bin[1], HONG Zhi[2,†]
(1 *Center for Optical and Electromagnetic Research, Zhejiang University, Hangzhou* 310058, *China*)
(2 *Center for Terahertz Research, China Jiliang University, Hangzhou* 310018, *China*)

Abstract: To overcome the disadvantage of low radiation power for photoconductive antenna, three types of antennas, including dipole, bow-tie and spiral antennas, are studied, where finite integration technology are used to compute their radiation impedances. The simulation results show that the impedance of dipole antenna is dependent on the dipole length, width, photoconductive gap and the width of transmission line, and has a peak value in resonant frequency, so the dipole antenna is suitable for applications working at specific terahertz frequency. The bow-tie and spiral antennas, known as broadband antennas, have approximately stable impedance over the terahertz frequency range under study. The simulation results also show that, the interdigitated fingers, which can be modelled as an additional capacitance, cause the antenna impedance to fall dramatically at high frequency.

Key words: Terahertz; Photomixing; Dipole antenna; Bow-tie antenna; Spiral antenna
CLCN: O431 **Document Code**: A **doi**: 10.3788/gzxb20103902.0233

0 Introduction

The terahertz (THz) region of the electromagnetic spectrum, typically considered to occupy 100 GHz to 10 THz, lies between microwave and infrared. Terahertz radiation can penetrate many materials with modest attenuation, and lots of chemical substances and explosive materials exhibit characteristic spectral responses at terahertz frequencies. Additionally, being at sub-millimeter wavelengths, it is of low energy and non-ionising. These unique properties make terahertz radiation a potentially powerful technique in the security screening[1-2], non-destructive testing[3], and medical imaging[4].

Photoconductive antennas, which can work at room temperature, are widely used in pulsed and continuous terahertz generation and detection[1,5-6]. As continuous-wave terahertz emitters, they are usually used as photomixers pumped by two light beams whose frequency difference is in the terahertz range. The output of terahertz beam has narrow linewidth, and wide range tunable properties, but the main restriction is their limited terahertz radiation power. The terahertz output power for photoconductive antenna is proportional to its radiation impedance according to photomixing principle[7-8]. Many researchers have performed optimization of antenna design to improve their radiation properties. Mclntosh, et al experimentally compared the output power from spiral antennas with different photoconductive gap areas[9]. Grogery, et al studied the terahertz emission from bow-tie antenna with bare gap and interdigitated fingers, and concluded that the terahertz output efficiency at high frequencies was additionally dependent on the design of photomixer fingers[10]. Theoretical methods were presented by Brown to evaluate the terahertz output power from photoconductive structures consisting of interdigitated electrodes[11]. The dependence of carrier lifetime and carrier velocity on the electric field was taken into account by Saeedkia, et al[12].

This paper systematically and theoretically studies three types of antennas with different mechanical designs, and compares their radiation impedances through simulation.

1 Photoconductive antennas

Three types of photoconductive antennas, including dipole antenna[8], bow-tie antenna[10,13] and spiral antenna[9,14], are studied in this paper. Fig. 1 shows the schematic diagrams of the three

* Supported by the National Natural Science Foundation of China (60576042)
† Tel: 0571-86845096 Email: hongzhi@cjlu.edu.cn
Received date: 2009-03-19 Revised date: 2009-05-07

kinds of photoconductive antennas. The dipole antenna with two designs of electrodes coupled to the external circuit is shown in Fig. 1(a), and an equivalent circuit, which is suitable for bow-tie and spiral antenna too, is given in Fig. 2.

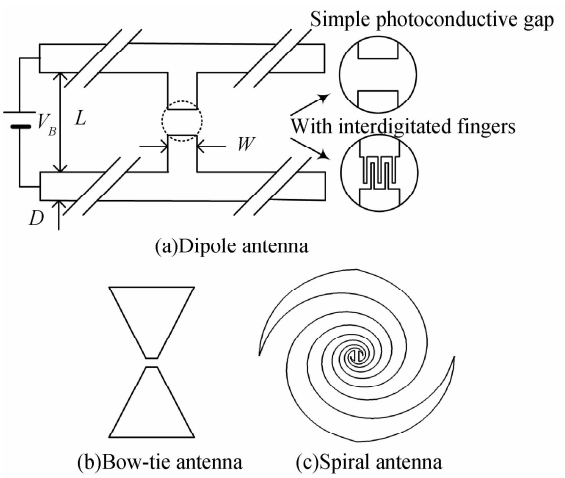

Fig. 1 Schematic diagrams of dipole antenna, bow-tie antenna and spiral antenna

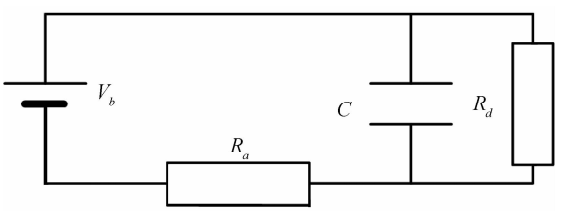

Fig. 2 Equivalent circuit for the biased photoconductive antenna

In the antenna design, there are two categories of photoconductive antennas, one with simple gap and the other with interdigitated fingers. In the former case, Ref [8] has demonstrated that the antenna length and width have effects on resonant frequency for dipole antenna. Photoconductive gap and transmission line width are the other main parameters for dipole antenna too. Bow-tie angle and turns of spiral affect the radiation properties for bow-tie antenna and spiral antenna, respectively.

Photomixing is a technique to generate continuous-wave terahertz radiation with photoconductive antennas. The procedure for photomixing proceeds as follows[11-12]. A bias photoconductive antenna fabricated on a semiconductor is illuminated with an optical beam. The optical beam generates free carriers in the photoconductive gap, when the photon energy of the optical beam is larger than the band gap of the semiconductor. If the carrier lifetime of the semiconductor is short enough under bias condition, it can respond to the current modulation in the photoconductive antenna. Terahertz radiation generates and is emitted into free space.

Continuous-wave terahertz emission occurs by illuminating the electrode gap with two single-mode continuous-wave laser beams, whose average power is P_1 and P_2, and angular frequency is ω_1 and ω_2, respectively. The instantaneous optical power incident on the antenna is given below [15]

$$P(w,t)=P_1+P_2+2\sqrt{mP_1P_2}\cos(\omega t+\varphi) \quad (1)$$

$$P_i=\int\left(cn\varepsilon_0\frac{E_i^2}{2}\right)\mathrm{d}S \quad (i=1,2,\omega=\omega_1-\omega_2) \quad (2)$$

where $P_i(i=1,2)$ are averaged powers of the two beams, c is the speed of light in vacuum, n is the refractive index of the media, ε_0 is the dielectric constant of vacuum, φ is the relative phase between the two optical beam, and m is the spatial-mixing efficiency of the two beams. The frequency difference of the two incident laser beams w can be tuned in the terahertz frequency range and the integration in equation (2) is carried out over the beam cross section.

The carrier density in the photoconductive gap is given by

$$\frac{\mathrm{d}n}{\mathrm{d}t}=\eta P(\omega,t)-\frac{n}{\tau} \quad (3)$$

where n is the photo-excited carrier number, η is the excitation efficiency, and τ is the photo-excited carrier lifetime.

Using the equivalent circuit diagram for the photoconductive antenna and the equation (3), the terahertz output power $P_{THz}(\omega)$ *is given by*

$$P_{THz}(\omega)=\frac{J_0^2R_a}{2[1+(\omega\tau)^2][1+(\omega R_aC)^2]} \quad (4)$$

where $J_0(=G_0V_b)$ is the DC photocurrent, G_0 is the time-averaged photoconductance for the average total incident power, V_b is the bias voltage, Ra is the radiation impedance of the antenna, and C is the capacitance of the photoconductive gap. $R_d=1/G$, where G is the photoconductance of the antenna.

Equation (4) shows that the terahertz output power is proportional to the radiation impedance of the antenna, and the square of DC conductance and bias voltage. Since the impedance of photoconductive antenna is important for continuous-wave terahertz radiation, the impedance characteristics of these above three types of photoconductive antennas are studied.

2 Simulation results

In the simulation, the impedances of different antennas are calculated numerically as a function of

frequency based on finite integration technique. The antenna geometries are firstly defined within a finite-element mesh and metal electrodes as perfect electrical conductors, and the terahertz radiation is modeled by generating a Gaussian terahertz wave in the photoconductive gap and examining the frequency-dependent current and voltage at the antenna feed. The antenna radiation impedance is calculated by monitoring the voltage and current within the antenna. Finally, the curves of impendence are plotted as a function of frequency.

Fig. 3 shows the results for dipole antennas with two different antenna lengths, where (a) is 40 μm and (b) is 80 μm. The parameters for dipole antennas in Fig. 3 are dipole length, dipole width, photoconductive gap and transmission line width. In Fig. 3, the Dipole Ⅰ 40/10/10/10 stands for a dipole antenna with dipole length 40 μm, dipole width 10 μm, photoconductive gap 10 μm and transmission line width 10 μm. The simulation results in 3(a) and 3(b) show fundamental resonant frequencies of about 0.85 THz and 0.76 THz, respectively, which have relatively high impedances of a few 1 000 Ω. Other weak resonant frequencies also exist when the dipole length becomes short enough. The resonant frequency moves towards higher frequency domain as the gap size becomes larger, where the resonant frequency for Dipole Ⅰ (0.86 THz) is higher than Dipole Ⅲ (0.84 THz). Moreover, the resonant impedance becomes smaller when the transmission line width becomes larger. It is shown from Fig. 3 that, the resonant frequency moves towards lower frequency domain when the dipole length becomes longer, which is consistent with the experimental results in ref [8]. However, even when the antenna length becomes very short, high resonant frequency can not be achieved[16]. The simulation results also show that the resonant frequency moves towards lower frequency domain as the dipole width becomes larger. The dipole antennas mentioned above are a kind of end-feed dipole antenna proposed by Gregory et al[16], the resonant frequency of which is inversely proportional to the dipole length. This conclusion is supported by the results of calculation.

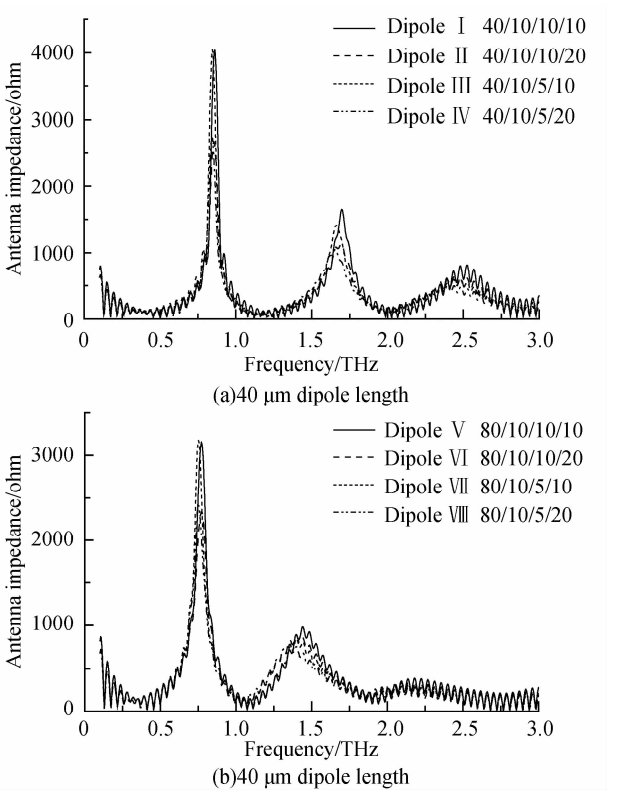

Fig. 3　Impedances of Dipole antennas

The parameters for bow-tie antenna are antenna length, bow-tie angle and photoconductive gap. It is shown in Fig. 4 that, the antenna impedance becomes lower as the bow-tie angle becomes larger, and the influence of photoconductive gap is evident at high frequency. Moreover, the bow-tie antenna has approximately stable impedance of about a few 100 Ω over the calculated frequency range.

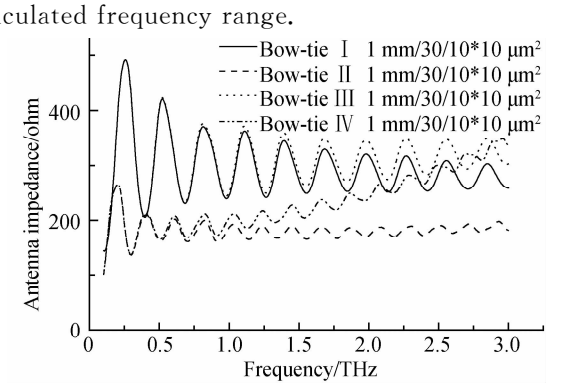

Fig. 4　Impedances of Bow-tie antennas

The spiral antennas under simulation is a kind of self-complimentary spiral with a constant impedance of 188.5 Ω for a semiconductor half-space[14]. Fig. 5 shows the simulation results for Spiral antenna Ⅰ, Ⅱ, Ⅲ, Ⅳ. The parameters for spiral antenna are turns of spiral and photoconductive gap. It can be concluded that, the impedance in high frequency domain becomes higher as the photoconductive gap becomes larger. Meanwhile, the turns of spiral has little effect on the impedance when the other parameters are the same. Fig. 5 indicates that spiral antenna is also a type of broadband antenna.

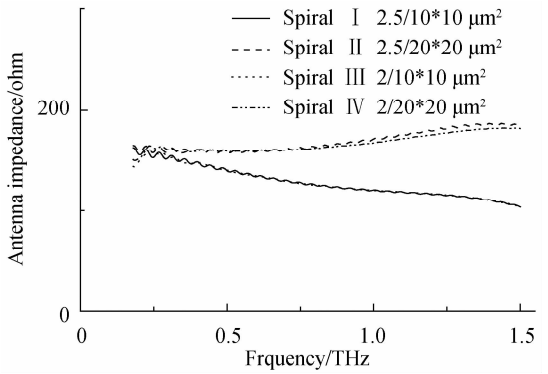

Fig. 5 Impedances of Spiral antennas

In the latter case of antenna design, the interdigitated fingers are modeled as a lumped capacitance in parallel with the photoconductive active area. Fig. 6 shows that the simulation results for three types of antennas with interdigitated fingers, the capacitances of which are about 1 fF[14] for the case of the active area of 100 μm^2, the electrode width of 0.5 μm and the width of the gap between the electrodes of 1.5 μm. Fig. 6(a) shows that fundamental resonant frequency still exist for the dipole antenna with interdigitated fingers, but the resonant frequency moves to lower and the radiation impedance decreases as the frequency goes up to 3 THz. For bow-tie antenna and spiral antenna, it can be seen in Fig. 6(b) and (c) that the additional capacitance of interdigitated fingers causes the antenna impedance to fall dramatically at frequency beyond 0.5 THz, which has been presented experimentally by Gregory and Brown et al. that the capacitive effect makes the radiation impedance fall apparently as the frequency increases[10,14].

The above simulations results show that, the dipole antenna has the property of high impedance, no less than a few thousand ohms around the fundamental resonant frequency, while the bow-tie and spiral antenna have stable impedance about a few hundred ohms over the calculated frequency range. As the terahertz radiant power is proportional to the antenna impedance, the magnitude of the resonant power for dipole antenna increases by up to an order of magnitude at the specific frequency, compared with broadband antennas such as bow-tie antenna and spiral antenna. In fact, remarkable improvement of terahertz output power has been achieved with high-impedance antenna designs as dual-dipole and dual-slot antennas[17].

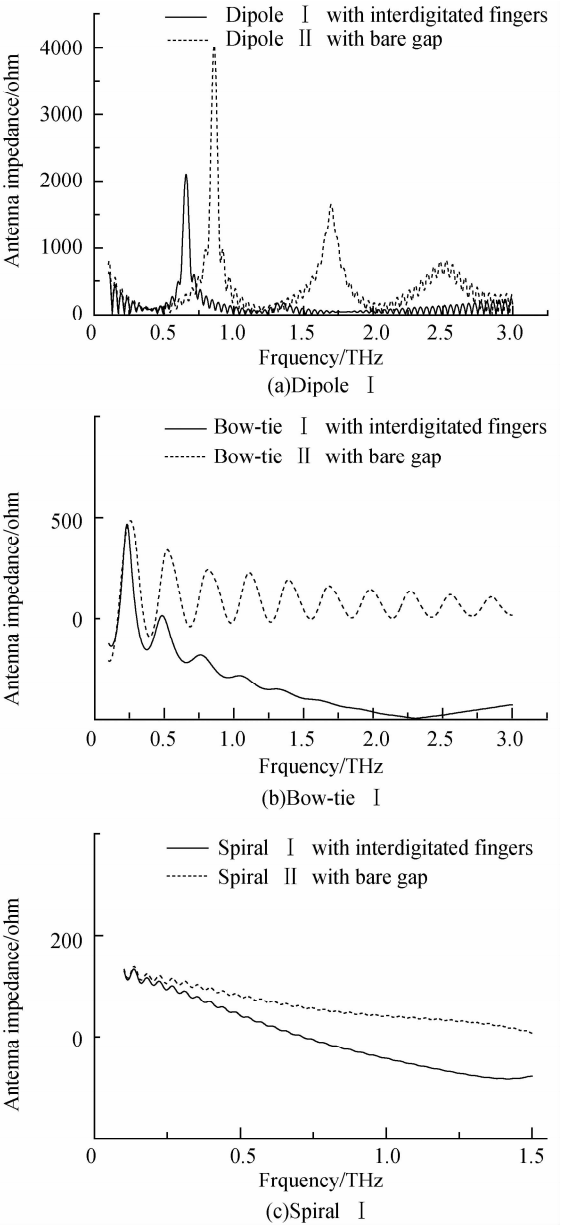

Fig. 6 Impedances of three kinds of antennas with and without interdigitated fingers

3 Conclusions

In summary, we have studied the impedance properties of three types of photoconductive antennas for continuous terahertz radiation. The results show that dipole antenna, as a kind of resonant antenna, has high radiation impedance around the resonant frequency, which can result in efficient terahertz radiation at some specific frequency. The bow-tie and spiral antennas are more suitable for broadband terahertz applications, because they have stable impedance over a quite broad frequency range. Moreover, the interdigitated fingers have effect on the three types of antennas at high frequencies. All the above antennas will be experimentally studied in our continuous-wave terahertz system in future.

References

[1] GREGORY I S, TRIBE W R, BAKER C, *et al*. Continuous-wave terahertz system with a 60 dB dynamic range [J]. *Appl Phys Lett*, 2005, **86**(20): 204104.

[2] XI Zai-jun, XIAO Ti-qiao, ZHANG Zeng-yan, *et al*. Investigation on two-dimensional transmission imaging with terahertz wave by time domain spectroscopy [J]. *Acta Photonica Sinica*, 2006, **35**(8): 1171-1174.

[3] MITTLEMAN D M, JACOBSEN R H, NUSS M C. T-ray imaging [J]. *IEEE J Selected Topics in Quantum Electronics*, 1996, **2**(3): 679-692.

[4] NAKAJIMA S, HOSHINA H, Yamashita M, *et al*. Terahertz imaging diagnostics of cancer tissues with a chemometrics technique [J]. *Appl Phys Lett*, 2007, **90**(4): 041102.

[5] JIA Wan-li, JI Wei-li, SHI Wei. Two-dimensional Monte Carlo simulation of screening of the bias field in terahertz generation from semi_insulated GaAs photoconductors [J]. *Acta Physica Sinica*, 2007, **56**(4): 2042-2046.

[6] LIU Ming-li, ZHANG Tong-yi, SUN Chuan-dong, *et al*. Characterization of high-power narrow-band terahertz radiation generation using large-aperture photoconductive antennas [J]. *Acta Photonica Sinica*, 2007, **36**(10): 1793-1798.

[7] TANI M, GU P, HYODO M, *et al*. Generation of coherent terahertz radiation by photomixing of dual-mode lasers [J]. *Opt Quantum Electron*, 2000, **32**(4): 503-520.

[8] MATSUURA S, TANI M, SAKAI K. Generation of coherent terahertz radiation by photomixing in dipole photoconductive antennas [J]. *Appl Phys Lett*, 1997, **70**(3): 559-561.

[9] MCINTOSH K A, BROWN E R, NICHOLS K B, *et al*. Terahertz photomixing with diode lasers in low-temperature-grown GaAs [J]. *Appl Phys Lett*, 1995, **67**(26): 3844-3846.

[10] GREGORY I S, BAKER C, TRIBE W R, *et al*. Optimization of photomixers and antennas for continuous-wave terahertz emission [J]. *IEEE J Quantum Electron*, 2005, **41**(5): 717-728.

[11] BROWN E R. A photoconductive model for superior GaAs THz photomixers [J]. *Appl Phys Lett*, 1999, **75**(6): 769-771.

[12] SAEEDKIA D, SAFAVI-NAEINI S. A comprehensive model for photomixing in ultrafast photoconductors [J]. *IEEE Photon Technol Lett*, 2006, **18**(13): 1457-1459.

[13] TANI M, MATSUURA S, SAKAI K, *et al*. Multiple-frequency generation of sub-terahertz radiation by multimode LD excitation of photoconductive antenna [J]. *IEEE Microwave and Guided Wave Lett*, 1997, **7**(9): 282-284.

[14] BROWN E R, MCINTOSH K A, NICHOLS K B, *et al*. Photomixing up to 3.8 THz in low-temperature-grown GaAs [J]. *Appl Phys Lett*, 1995, **66**(3): 285-287.

[15] TANI M, MORIKAWA O, Matsuura S, *et al*. Generation of terahertz radiation by photomixing with dual- and multiple-mode lasers [J]. *Semicond Sci Technol*, 2005, **20**(7): S151-S163.

[16] GREGORY I S, TRIBE W R, COLE B E, *et al*. Resonant dipole antennas for continuous-wave terahertz photomixers [J]. *Appl Phys Lett*, 2004, **85**(9): 1622-1624.

[17] DUFFY S, VERGHESE S, MCINTOSH K, *et al*. Accurate modeling of dual dipole and slot elements used with photomixers for coherent terahertz output power [J]. *IEEE Trans Microwave Theory and Tech*, 2001, **49**(6): 1032-1038.

光电导天线辐射阻抗特性模拟分析

徐英[1]，陈海滨[1]，洪治[2]

(1 浙江大学 光及电磁波研究中心，杭州 310058)

(2 中国计量学院 太赫兹技术与应用研究所，杭州 310018)

摘　要：针对连续太赫兹光电导天线辐射功率较低的缺点，利用有限积分方法对三种常用的光电导天线，包括偶极天线、蝶形天线和螺旋天线，进行数值模拟并分析比较其辐射阻抗特性. 仿真结果表明，偶极天线的辐射阻抗与偶极长度、宽度、电极间隙以及传输线宽度有关，且在其谐振频率存在峰值阻抗，适用于特定频率的太赫兹波辐射. 蝶形天线和螺旋天线在所研究的太赫兹波段具有近似稳定的辐射阻抗，广泛应用于宽带领域. 对带有交叉电极的电极间隙进行计算，结果表明由交叉电极引入的附加电容降低了天线的高频阻抗.

关键词：太赫兹；光子混频；偶极天线；蝶形天线；螺旋天线

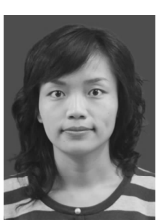

XU Ying　was born in 1982. Now she is pursuing her Ph. D. degree from Department of Opitcal Engineering, Zhejiang University. Her research interests focus on photoconductive antenna and continuous-wave terahertz system.

HONG Zhi　was born in 1964. He received the Ph. D. degree in optical engineering from Zhejiang University in 2001. Now he is a professor and director of Centre for Terahertz Research, China Jiliang University, and his main research interests focus on terahertz device, sensing, and imaging; lasers; quantum information processing.